



## Beyond Reuse Distance Analysis: Dynamic Analysis for Characterization of Data Locality Potential

Naznin Fauzia, Venmugil Elango, Mahesh Ravishankar, Jagannathan Ramanujam, Fabrice Rastello, Atanas Rountev, Louis-Noël Pouchet, Ponnuswamy Sadayappan

### ► To cite this version:

Naznin Fauzia, Venmugil Elango, Mahesh Ravishankar, Jagannathan Ramanujam, Fabrice Rastello, et al.. Beyond Reuse Distance Analysis: Dynamic Analysis for Characterization of Data Locality Potential. Transaction on Architecture and Code Optimization, ACM, 2013, 10 (4). <hal-00920031>

**HAL Id: hal-00920031**

**<https://hal.inria.fr/hal-00920031>**

Submitted on 20 Dec 2013

**HAL** is a multi-disciplinary open access archive for the deposit and dissemination of scientific research documents, whether they are published or not. The documents may come from teaching and research institutions in France or abroad, or from public or private research centers.

L'archive ouverte pluridisciplinaire **HAL**, est destinée au dépôt et à la diffusion de documents scientifiques de niveau recherche, publiés ou non, émanant des établissements d'enseignement et de recherche français ou étrangers, des laboratoires publics ou privés.



# Beyond Reuse Distance Analysis: Dynamic Analysis for Characterization of Data Locality Potential\*

*Naznin Fauzia<sup>1</sup>, Venmugil Elango<sup>1</sup>, Mahesh Ravishankar<sup>1</sup>, J. Ramanujam<sup>2</sup>,  
Fabrice Rastello<sup>3</sup>, Atanas Rountev<sup>1</sup>, Louis-Noël Pouchet<sup>4</sup>, P. Sadayappan<sup>1</sup>*

1: The Ohio State University   2: Louisiana State University   3: INRIA / LIP, ENS Lyon   4: University of California Los Angeles

## Abstract

Emerging computer architectures will feature drastically decreased flops/byte (ratio of peak processing rate to memory bandwidth) as highlighted by recent studies on Exascale architectural trends. Further, flops are getting cheaper while the energy cost of data movement is increasingly dominant. The understanding and characterization of data locality properties of computations is critical in order to guide efforts to enhance data locality.

Reuse distance analysis of memory address traces is a valuable tool to perform data locality characterization of programs. A single reuse distance analysis can be used to estimate the number of cache misses in a fully associative LRU cache of any size, thereby providing estimates on the minimum bandwidth requirements at different levels of the memory hierarchy to avoid being bandwidth bound. However, such an analysis only holds for the particular execution order that produced the trace. It cannot estimate potential improvement in data locality through dependence preserving transformations that change the execution schedule of the operations in the computation.

In this article, we develop a novel dynamic analysis approach to characterize the inherent locality properties of a computation and thereby assess the potential for data locality enhancement via dependence preserving transformations. The execution trace of a code is analyzed to extract a computational directed acyclic graph (CDAG) of the data dependences. The CDAG is then partitioned into convex subsets, and the convex partitioning is used to reorder the operations in the execution trace to enhance data locality. The approach enables us to go beyond reuse distance analysis of a single specific order of execution of the operations of a computation in characterization of its data locality properties. It can serve a valuable role in identifying promising code regions for manual transformation, as well as assessing the effectiveness of compiler transformations for data locality enhancement. We demonstrate the effectiveness of the approach using a number of benchmarks, including case studies where the potential shown by the analysis is exploited to achieve lower data movement costs and better performance.

## 1 Introduction

Advances in technology over the last few decades have yielded significantly different rates of improvement in the computational performance of processors relative to the speed of memory access. The Intel 80286 processor introduced in 1982 had an operation execution latency of 320 ns and a main memory access time of 225 ns [15]. The recent Intel Core i7 processor has an operation latency of 4ns and a memory latency of 37 ns, illustrating an order of magnitude shift in the ratio of operation latency to memory access latency. Since processors use parallelism and pipelining in execution of operations and for memory access, it is instructive to also examine the trends in the peak execution throughput and memory bandwidth for these two processors: 2 MIPS and 13 MBytes/sec for the 80286 versus 50,000 MIPS and 16,000 MBytes/sec for the Core i7. The ratio of peak computational rate to peak memory access bandwidth has also changed by more than an order of magnitude.

Because of the significant mismatch between computational latency and throughput when compared to main memory latency and bandwidth, the use of hierarchical memory systems and the exploitation of significant data reuse in the higher (i.e., faster) levels of the memory hierarchy is critical for high performance. Techniques such as pre-fetching

---

\*This work is supported in part by the U.S. National Science Foundation through awards 0811457, 0904549, 0926127, 0926687, 0926688 and 1321147, by the U.S. Department of Energy through award DE-SC0008844, and by the U.S. Army through contract W911NF-10-1-000.

and overlap of computation with communication can be used to mitigate the impact of high memory access latency on performance, but the mismatch between maximum computational rate and peak memory bandwidth is much more fundamental; *the only solution is to limit the volume of data movement to/from memory by enhancing data reuse in registers and higher levels of the cache.*

A significant number of research efforts have focused on improving data locality, by developing new algorithms such as the so called *communication avoiding* algorithms [3, 4, 10] as well as automated compiler transformation techniques [7, 18, 22, 49]. With future systems, the cost of data movement through the memory hierarchy is expected to become even more dominant relative to the cost of performing arithmetic operations [5, 13, 41], both in terms of throughput and energy. Optimizing data access costs will become ever more critical in the coming years. Given the crucial importance of optimizing data access costs in systems with hierarchical memory, it is of great interest to develop tools and techniques to assess the inherent data locality characteristics of different parts of a computation, and the potential for data locality enhancement via dependence preserving transformations.

Reuse distance (also called LRU stack distance) is a widely used approach to model data locality [11, 30] in computations. Since its introduction in 1970 by Mattson et al. [30], reuse distance analysis has found numerous applications in performance analysis and optimization, such as cache miss rate prediction [20, 29, 52], program phase detection [42], data layout optimization [53], virtual memory management [9] and I/O performance optimization [19]. Defined as the number of distinct memory references between two successive references to the same location, reuse distance provides a quantification of the locality present in a data reference trace. A key property of the reuse distance characterization of an address trace is that, for a fully associative cache of size  $S$ , every reference with reuse distance  $d \leq S$  would be a hit and all others misses. Thus, a single reuse distance analysis of an address trace allows to estimate the total number of hits/misses for an idealized cache of any size, from a cumulative reuse distance histogram. In contrast, cache simulation to determine the number of hits/misses would have to be repeated for each cache size of interest. Although real caches have non-unit line size and finite associativity, the data transfer volume estimated from the cache miss count via reuse distance analysis can serve as a valuable estimate for any real cache.

Although reuse distance analysis has found many uses in characterizing data locality in computations, it has a fundamental constraint: *The analysis is based on the memory address trace corresponding to a particular execution order of the operations constituting the computation.* Thus, it does not in any way account for the possibility of alternate valid execution orders for the computation that may exploit much better data locality. While reuse distance analysis provides a useful characterization of data locality for a given execution trace, it fails to provide any information on the potential for improvement in data locality that may be feasible through valid reordering of the operations in the execution trace. In particular, given only the reuse distance profile for the address trace generated by execution of some code, it is not possible to determine whether the observed locality characteristics reveal fundamental inherent limitations of an algorithm, or are merely the consequence of a sub-optimal implementation choice.

In this paper, we develop a novel dynamic analysis approach to provide insights beyond that possible from standard reuse distance analysis. The analysis seeks to characterize the *inherent data locality potential* of the implemented algorithm, instead of the reuse distance profile of the address trace from a specific execution order of the constituent operations. We develop graph partitioning techniques that could be seen as a generalization of loop tiling, but considering arbitrary shapes for the tiles that enable atomic execution of tiles. Instead of simply performing reuse distance analysis on the execution trace of a given sequential program, we first explicitly construct a computational directed acyclic graph (CDAG) to capture the statement instances and their inter-dependences, then perform convex partitioning of the CDAG to generate a modified dependence-preserving execution order with better expected data reuse, and finally perform reuse distance analysis for the address trace corresponding to the modified execution order. We apply the proposed approach on a number of benchmarks and demonstrate that it can be very effective. This article makes the following contributions.

- It is the first work, to the best of our knowledge, to develop a dynamic analysis approach that seeks to characterize the inherent data locality characteristics of algorithms.
- It develops effective algorithms to perform convex partitioning of CDAGs to enhance data locality. While convex partitioning of DAGs has previously been used for estimating parallel speedup, to our knowledge this is the first effort to use it for characterizing data locality potential.
- It demonstrates the potential of the approach to identify opportunities for enhancement of data locality in existing

implementations of computations. Thus, an analysis tool based on this approach to data locality characterization can be valuable to: (i) application developers, for comparing alternate algorithms and identifying parts of existing code that may have significant potential for data locality enhancement, and (ii) compiler writers, for assessing the effectiveness of a compiler’s program optimization module in enhancing data locality.

- It demonstrates, through case studies, the use of the new dynamic analysis approach in identifying opportunities for data locality optimization that are beyond the scope of the current state-of-the-art optimizing compilers. For example, the insights from the analysis have resulted in the development of a 3D tiled version of the Floyd-Warshall all-pairs shortest paths algorithm, which was previously believed to be un-tileable without semantic information of the base algorithm.

The rest of the paper is organized as follows. Section 2 presents background on reuse distance analysis, and a high-level overview of the proposed approach for locality characterization. The algorithmic details of the approach to convex partitioning of CDAGs are provided in Section 3. Section 4 presents experimental results. Related work is discussed in Section 5, followed by concluding remarks in Sections 6 and 7.

## 2 Background & Overview of Approach

### 2.1 Reuse Distance Analysis

Reuse distance analysis is a widely used metric that models data locality [11, 30]. The reuse distance of a reference in a memory address trace is defined as the number of distinct memory references between two successive references to the same location.

Time	0	1	2	3	4	5	6	7	8	9
Data Ref.	d	a	c	b	c	c	e	b	a	d
Reuse Dist.	$\infty$	$\infty$	$\infty$	$\infty$	1	0	$\infty$	2	3	4

Fig. 1: Example data reference trace

An example data reference trace of length  $N = 10$  is shown in Fig. 1. It contains references to  $M = 5$  distinct data addresses  $\{a, b, c, d, e\}$ . As shown in the figure, each reference to an address in the trace is associated with a reuse distance. The first time an address is referenced, its reuse distance is  $\infty$ . For all later references to an address, the reuse distance is the number of distinct intervening addresses referenced. In the figure, address  $c$  is referenced three times. Since  $b$  is referenced in between the first and second references to  $c$ , the latter has a reuse distance of 1. Since the second and third references to  $c$  are consecutive, without any other distinct intervening references to any other addresses, the last access to  $c$  has a reuse distance of 0.

A significant advantage of reuse distance analysis (RDA) is that a single analysis of the address trace of a code’s execution can be used to estimate data locality characteristics as a function of the cache size. Given an execution trace, a reuse distance histogram for that sequence is obtained as follows. For each memory reference,  $M$  in the trace, its reuse distance is the number of distinct addresses in the trace after the most recent access to  $M$  (the reuse distance is considered to be infinity if there was no previous reference in the trace to  $M$ ). The number of references in the trace with reuse distance of 0, 1, 2, ..., are counted to form the reuse distance histogram. A cumulative reuse distance histogram plots, as a function of  $k$ , the number of references in the trace that have reuse distance less than or equal to  $k$ . The cumulative reuse distance histogram directly provides the number of cache hits for a fully associative cache of capacity  $C$  with a LRU (Least Recently Used) replacement policy, since the data accessed by any reference with reuse distance less than or equal to  $C$  would result in a cache hit.

**Example** We use a simple example to illustrate both the benefits as well as a significant limitation of standard RDA. Fig. 2 shows code for a simple Seidel-like spatial sweep, with a default implementation and a fully equivalent tiled variant, where the computation is executed in blocks.

```

for(i = 1; i < N-1; i++)
  for(j = 1; j < N-1; j++)
    A[i][j] = A[i-1][j] + A[i][j-1];

```

```

/* B -> Tile size */
for(it = 1; it < N-1; it += B)
  for(jt = 1; jt < N-1; jt += B)
    for(i = it; i < min(it+B, N-1); i++)
      for(j = jt; j < min(jt+B, N-1); j++)
        A[i][j] = A[i-1][j] + A[i][j-1];

```

Fig. 2: Example: Single-sweep two-point Gauss-Seidel code, (a) Untiled and (b) Tiled

Fig. 3(a) displays the cumulative reuse distance histogram for both versions. As explained above, it can be interpreted as the number of data cache hits (y axis) as a function of the cache size (x axis). The same data is depicted in Fig. 3(b), showing the number of cache misses (by subtracting the number of hits from the total number of references). untiled form of the code, a cache with capacity less than 400 words (3200 bytes, with 8 bytes per element) will be too small to effectively exploit reuse. The reuse distance profile for the tiled code is quite different, suggesting that effective exploitation of reuse is feasible with a smaller cache of capacity of 50 words (400 bytes). This example illustrates the benefits of RDA: i) For a given code, it provides insights into the impact of cache capacity on the expected effectiveness of data locality exploitation, and ii) Given two known alternative implementations for a computation, it enables a comparative assessment of the codes with respect to data locality.

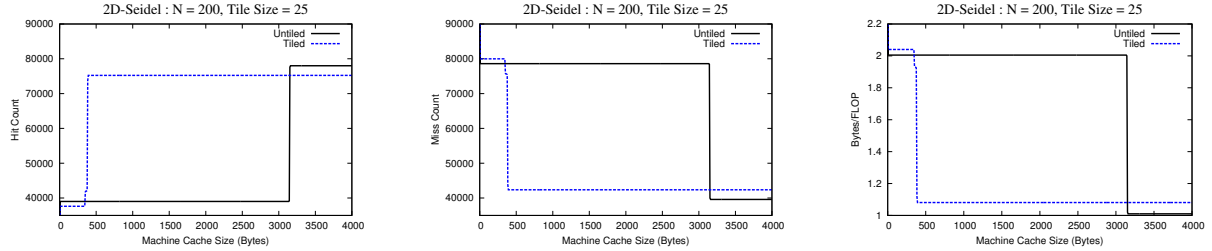


Fig. 3: Reuse distance profile: (a) cache hit rate, (b) cache miss rate, and (c) memory bandwidth demand for tiled/untiled versions of code in Fig. 2

**Limitations of reuse distance analysis** The Seidel example also illustrates a fundamental shortcoming of RDA that we address through the work presented in this article: Given an execution trace for a code, RDA only provides a data locality characterization for one *particular execution order* of the constituent operations, and provides no insights on whether significant improvements may be possible via dependence preserving reordering of execution of the operations. The tiled and untiled variants in Fig. 2 represent equivalent computations, with the only difference being the relative order of execution of exactly the same set of primitive arithmetic operations on exactly the same sets of array operands. Although state-of-the-art static compiler transformation techniques (e.g., using polyhedral loop transformations) can transform the untiled code in Fig. 2(a) to a tiled form of Fig. 2(b), many codes exist (as illustrated through case studies later in this article), where data locality characteristics can be improved, but are beyond the scope of the most advanced compilers today. The main question that RDA does not answer is whether the poor reuse distance profile for the code due to a sub-optimal execution order of the operations (e.g., untiled code version of a tileable algorithm) or is it more fundamental property of the computation that remains relatively unchangeable through any transformations that change the execution order of the operations? This is the question our work seeks to assist in answering. By analyzing the execution trace of a given code, forming a dynamic data dependence graph, and reordering the operations by forming convex partitions, the potential for improving the reuse distance profile is evaluated. The change to the reuse distance profile after the dynamic analysis and reordering, rather than the shape of the initial reuse distance profile of a code, provides guidance on the potential for further improvement.

Fig. 3(c) presents the information in Fig. 3(b) in terms of memory bandwidth required per operation. It translates the cache miss count into the bandwidth demand on the memory system in bytes/second per floating-point operation.

For this code, we have one floating point operation per two memory references. With a cache miss rate  $m$ , assuming double-precision (8 bytes per word), the demand on the main-memory bandwidth would be  $16 * m$  bytes per Flop. If this ratio is significantly higher than the ratio of a system’s main memory bandwidth (in Gbytes/sec) to its peak performance (in GFlops), the locality analysis indicates that achieving high performance will be critically dependent on effective data locality optimization. For example, on most current systems, the performance of this computation will be severely constrained by main memory bandwidth for problem sizes that are too large to fit in cache.

A point of note is that while the estimated cache hit rates/counts by using RDA can deviate quite significantly from actually measured cache hit rates/counts on real systems (due to a number of aspects of real caches, such as non-unit line size, finite associativity, pre-fetching, etc.), the bytes/flop metric serves as a good indicator of the bandwidth requirement for real caches. This is because pre-fetching and non-unit line sizes only affect the latency and number of main memory accesses and not the minimum volume of data that must be moved from memory to cache. Finite cache associativity could cause an increase in the number of misses compared to a fully associative cache, but not a decrease. All the experimental results presented later in the article depict estimates on the bytes/flop bandwidth demanded by a code. Thus, despite the fact that RDA essentially models an idealized fully associative cache, the data represents useful estimates on the bandwidth demand for any real cache.

**Benefits of the proposed dynamic analysis** Using results from two case studies presented later in the article, we illustrate the benefits of the approach we develop. Fig. 4 shows the original reuse distance profiles as well as the profiles after dynamic analysis and convex partitioning, for two benchmarks: Householder transformation on the left, and Floyd-Warshall all-pairs shortest path on the right. As seen in the left plot in Fig. 4, with the Householder code, no appreciable change to the reuse distance profile results from the attempted reordering after dynamic analysis. In contrast, the right plot in Fig. 4 shows a significantly improved reuse distance profile for the Floyd-Warshall code, after dynamic analysis and reordering of operations. This suggests potential for enhanced data locality via suitable code transformations. As explained later in the experimental results section, manual examination of the convex partitions provided insights into how the code could be transformed into an equivalent form that in turn could be tiled by an optimizing compiler. The reuse distance profile of that tiled version is shown as a third curve in the right plot in Fig. 4, showing much better reuse than the original code. The actual performance of the modified code was also significantly higher than the original code. To the best of our knowledge, this is the first 3D tiled implementation of the Floyd Warshall algorithm (other blocked versions have been previously developed [34, 47], but have required domain-specific reasoning for semantic changes to form equivalent algorithms that generate different intermediate values but the same final results as the standard algorithm).

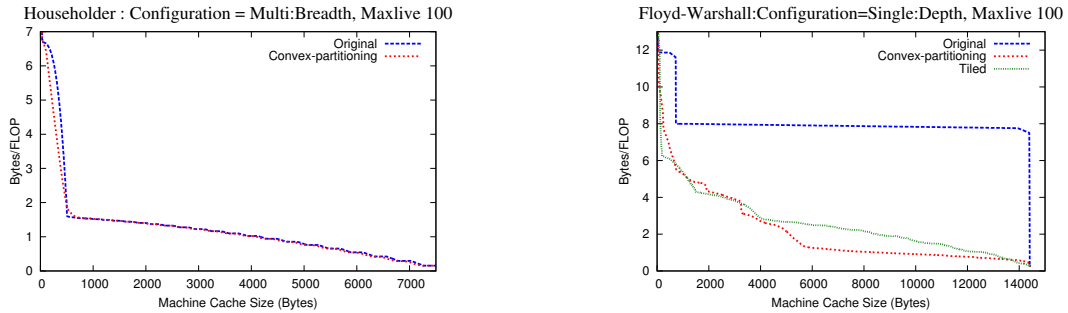


Fig. 4: Reuse distance analysis for Householder and Floyd-Warshall

## 2.2 Overview of Approach

The new dynamic analysis approach proposed in this paper attempts to characterize the inherent data locality properties of a given (sequential) computation, and to assess the potential for enhancing data locality via change of execution ordering. To achieve this goal, we proceed in two stages. First, a new ordering of the program’s operations is computed, by using graph algorithms (that is, convex partitioning techniques) operating on the expanded computation graph.

Then, standard reuse distance analysis is performed on the reordered set of operations. We note that our analysis does not directly provide an optimized program. Implementing the (possibly very complex) schedule found through our graph analysis is impractical. Instead, our analysis highlights gaps between the reuse distance profile of a current implementation and existing data locality potential: the task of devising a better implementation is left to the user or compiler writer. In Sec. 4, we show the benefits of the approach on several benchmarks.

To implement our new dynamic analysis, we first analyze the data accesses and dependences between the primitive operations in a sequential execution trace of the program to extract a more abstract model of the computation: a computational directed acyclic graph (CDAG), where operations are represented as vertices and the flow of values between operations as edges. This is defined as follows.

**CDAG [6]** A computation directed acyclic graph (CDAG) is a 4-tuple  $C = (I, V, E, O)$  of finite sets such that: (1)  $I \cap V = \emptyset$ ; (2)  $E \subseteq (I \cup V) \times V$  is the set of arcs; (3)  $G = (I \cup V, E)$  is a directed acyclic graph with no isolated vertices; (4)  $I$  is called the input set; (5)  $V$  is called the operation set and all its vertices have one or two incoming arcs; (6)  $O \subseteq (I \cup V)$  is called the output set.

Fig. 5 shows the CDAG corresponding to the code in Fig. 2 for  $N=6$  — both versions have identical CDAGs since they perform exactly the same set of floating-point computations, with the same inter-instance data dependences, even though the total order of execution of the statement instances is different. The loop body performs only one addition and is executed a total of 16 times, so the CDAG has 16 computation nodes (white circles).

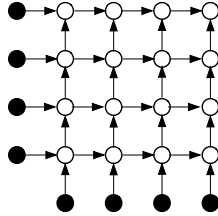


Fig. 5: CDAG for Gauss-Seidel code in Fig. 2. Input vertices are shown in black, other vertices represent operations performed.

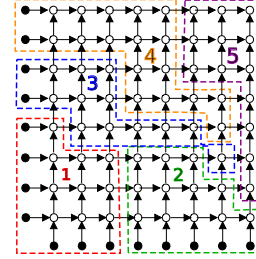


Fig. 6: Convex-partition of the CDAG for the code in Fig. 2 for  $N = 10$ .

Although a CDAG is derived from analysis of dependences between instances of statements executed by a sequential program, it abstracts away that sequential schedule of operations and only imposes an essential partial order captured by the data dependences between the operation instances. Control dependences in the computation need not be represented since the goal is to capture the inherent data locality characteristics based on the set of operations that were actually execution in the program.

The key idea behind the work presented in this article is to perform analysis on the CDAG of a computation, attempting to find a different order of execution of the operations that can improve the reuse-distance profile compared to that of the given program's sequential execution trace. If this analysis reveals a significantly improved reuse distance profile, it suggests that suitable source code transformations have the potential to enhance data locality. On the other hand, if the analysis is unable to improve the reuse-distance profile of the code, it is likely that it is already as well optimized for data locality as possible. The dynamic analysis involves the following steps:

1. Generate a sequential execution trace of a program.
2. Run a reuse-distance analysis of the original trace.
3. Form a CDAG from the execution trace.
4. Perform a multi-level convex partitioning of the CDAG, which is then used to change the schedule of operations of the CDAG from the original order in the given input code. A convex partitioning of a CDAG is analogous to tiling the iteration space of a regular nested loop computation. Multi-level convex partitioning is analogous to multi-level cache-oblivious blocking.



5. Perform standard reuse distance analysis of the reordered trace after multi-level convex partitioning.

Finally, Fig. 6 shows the convex partitioning of the CDAG corresponding to the code in Fig. 2.

After such a partitioning, the execution order of the vertices is reordered so that the convex partitions are executed in some valid order (corresponding to a topological sort of a coarse-grained inter-partition dependence graph), with the vertices within a partition being executed in the same relative order as the original sequential execution. Details are presented in the next section.

### 3 Convex Partitioning of CDAG

In this section, we provide details on our algorithm for convex partitioning of CDAGs, which is at the heart of our proposed dynamic analysis. In the case of loops, numerous efforts have attempted to optimize data locality by applying loop transformations, in particular involving loop tiling and loop fusion [7, 18, 22, 49]. Tiling for locality attempts to group points in an iteration space of a loop into smaller blocks (tiles) allowing reuse (thereby reducing reuse distance) in multiple directions when the block fits in a faster memory (registers, L1, or L2 cache). Forming a valid tiling for a loop requires that each tile can be executed atomically, i.e., each tile can start after performing required synchronizations for the data it needs, then execute all the iterations in the tile without requiring intervening synchronization. This means that there are no cyclic data dependencies between any two tiles. *Our goal in this work is to extend this notion of “tiling” to arbitrary CDAGs that represent a computation: we form valid partitioning of CDAGs into components such that the components can be scheduled and executed, with all vertices in a component being executed “atomically,” i.e., without being interleaved with vertices in any other components.* For this, we rely on the notion of *convex partitioning* of CDAGs, which is the generalization of loop tiling to graphs.

#### 3.1 Definitions

We first define what is a convex component, that is a tile in a graph.

**Convex component** Given a CDAG  $G$ , a convex component  $V_i$  in  $G$  is defined as a subset of the vertices of  $G$  such that, for any pair of vertices  $u$  and  $v$  in  $V_i$ , if there are paths between  $u$  and  $v$  in  $G$ , then every vertex on every path between  $u$  and  $v$  also belongs to  $V_i$ .

A convex partition of a graph  $G$  is obtained by assigning each vertex of  $G$  to a single convex component. Since there are no cycles among convex components, the graph in which nodes are convex components and edges define dependences among them, is acyclic. Therefore, we can execute the convex components using any topologically sorted order. Executing all the convex components results in executing the full computation.

A *convex partition* of a graph  $G = (V, E)$  is a collection of convex components  $\{V_1, \dots, V_k\}$  of  $G$  such that  $\bigcup_{i=1}^k V_i = V$  and for any  $i, j$  s.t.  $1 \leq i, j \leq k$  and  $i \neq j$ ,  $V_i \cap V_j = \emptyset$ . We remark that tiling of iterations spaces of loops results in convex partitions.

The *component graph*  $C = (\mathcal{V}_C, \mathcal{E}_C)$  is defined as a graph whose vertices  $\mathcal{V}_C$  represent the convex components, i.e.,  $\mathcal{V}_C = \{V_1, \dots, V_k\}$ . Given two distinct components  $V_i$  and  $V_j$ , there is an edge in  $C$  from  $V_i$  to  $V_j$  if and only if there is an edge  $(a, b)$  in the CDAG, where  $a \in V_i$  and  $b \in V_j$ .

For a given schedule of execution of the vertices of convex component  $V_i$ , we define *maxlive* to be the maximum number of simultaneously live nodes for this schedule. A node can be in one of the following states throughout its life: (*initial state*) at the beginning no node is live; (*birth*) any node is considered live right after it is fired (executed); (*resurrection*) if not part of the convex component, it is also considered as live when used by another node of the component (predecessor of a fired node belonging to the component); (*live*) a born or resurrected node stays alive until it dies, which happens if all its successor nodes have executed (are part of the partition); (*death*) a node dies right after its last successor fires.

Our goal is to form convex components along with a scheduling such that the *maxlive* of each component does not exceed the local memory capacity. We consider the nodes we add to the component (just fired and alive), and their predecessors (resurrected) in computing the *maxlive*.

### 3.2 Forming Convex Partitions

We show in Algorithm 1 our technique to build convex partitions from an arbitrary CDAG. It implements a convex-component growing heuristic that successively adds ready vertices into the component until a capacity constraint is exceeded. The key requirement in adding a new vertex to a convex component is that if any path to that vertex exists from a vertex in the component, then all vertices in that path must also be included. We avoid an expensive search for such paths by constraining the added vertices to be those that already have all their predecessors in the current (or previously formed) convex component.

---

**ALGORITHM 1:** GenerateConvexComponents( $G, C, CF$ )

---

**Input :**  $G$  : CDAG;  $C$  : Cache Size;

$CF$ : Cost function to decide next best node

**InOut:**  $P$  : Partition containing convex components

**begin**

```

 $P \leftarrow \emptyset$ 
 $R \leftarrow \text{getTheInitialReadyNodes}(G)$ 
while  $R \neq \emptyset$  do
     $n \leftarrow \text{selectReadyNode}(R)$ 
     $cc \leftarrow \emptyset$ 
    while  $R \neq \emptyset \wedge \text{updateLiveSet}(cc, n, C)$  do
         $cc \leftarrow cc \cup \{n\}$ 
         $R \leftarrow R - \{n\}$ 
         $\text{UpdateListOfReadyNodes}(R, n)$ 
         $priority \leftarrow CF()$ 
         $n \leftarrow \text{selectBestNode}(R, cc, priority, n)$ 
     $P \leftarrow P \cup \{cc\}$ 

```

---

The partitioning heuristic generates a valid schedule as it proceeds. At the beginning, all input vertices to the CDAG are placed in a ready list  $R$ . A vertex is said to be *ready* if all its predecessors (if any) have already executed, i.e., have been assigned to some convex component. A new convex component  $cc$  is started by adding a ready vertex to it (the function  $\text{selectReadyNode}(R)$  simply picks up one element of  $R$ ) and it grows by successively adding more ready nodes to it ( $\text{selectBestNode}(R, cc, priority, n)$  selects one of the ready nodes, as shown in Algorithm 4 – the criterion is described later). Suppose a vertex  $n$  is just added to a component  $cc$ . As a result, zero or more of the successors of  $n$  in  $G$  may become ready: a successor  $s$  of  $n$  becomes ready if the last predecessor needed to execute  $s$  is  $n$ . The addition of newly readied vertices to the ready list is done by the function  $\text{updateListOfReadyNodes}(R, n)$ , as shown in Algorithm 2. In this function, the test that checks if  $s$  has unprocessed predecessors is implemented using a counter that is updated whenever a node is processed.

---

**ALGORITHM 2:** UpdateListOfReadyNodes( $R, n$ )

---

**Input :**  $n$ : Latest processed node

**InOut:**  $R$ : List of ready nodes

**begin**

```

for  $s \in \text{successors}(n)$  do
    if  $s$  has no more unprocessed predecessors then
         $R \leftarrow R \cup \{s\}$ 

```

---

Before adding a node to  $cc$ , the set  $cc.liveset$ , the liveout set of  $cc$ , is updated through the call to  $\text{updateLiveSet}(p, n, C)$ , as shown in Algorithm 3.  $\text{updateLiveSet}$  exactly implements our definition of liveness previously described: (*birth*) if  $n$  has some successors it is added to the liveset of  $cc$ ; (*resurrect*) its predecessor nodes that still have unprocessed successors are added to the liveset (if not already in it); (*die*) predecessor nodes for which  $n$  is the last unprocessed successor are removed from the liveset.

---

**ALGORITHM 3:** updateLiveSet( $p, n, C$ )

---

**Input** :  $n$  : New node added in the partition  $p$   
           $C$  : Cache size

**InOut** :  $p.liveset$  : Live set of  $p$

**Output**: true if  $|p.liveset| \leq C$ , false otherwise

**begin**

```
   $lset \leftarrow p.liveset$ 
  if  $n$  has unprocessed successors then
     $p.liveset \leftarrow p.liveset \cup \{n\}$ 
  for  $n' \in \text{predecessors}(n)$  do
    if  $n'$  has unprocessed successors then
       $p.liveset \leftarrow p.liveset \cup \{n'\}$ 
    else if  $n' \in p.liveset$  then
       $p.liveset \leftarrow p.liveset - \{n'\}$ 
  if  $|p.liveset| > C$  then
     $p.liveset \leftarrow lset$ 
    return false
  return true
```

---

### 3.3 CDAG Traversal: Breadth-first Versus Depth-first

The heuristic `selectBestNode` to select the next processed node within the ready list uses two affinity notions: a node is a ready-successor of  $cc$  (thus element of the  $cc.readySuccessors$  list) if it is a ready successor of some nodes of  $cc$ ; a node is a ready-neighbor of  $cc$  (thus element of  $cc.readyNeighbors$  list) if it has a successor node that is also a successor of some node in  $cc$ . We note that those two lists can overlap. The growing strategy picks up ready nodes, using a first-in first-out policy, from one of those two lists. In practice, we observe that favoring nodes of the ready-successor list would favor growing depth-first in the CDAG, while favoring nodes that belongs to the ready-neighbor list would favor a breadth-first traversal.

The heuristic uses a combination of growing alternately in these two different directions till the *Maxlive* of the component exceeds the capacity of the cache. The priority is controlled by a number that represents the ratio of selected ready-neighbors over selected ready-successors. If the ratio is larger than 1, we refer to it as *breadth-priority*; if lower than 1, we refer to it as *depth-priority*, otherwise it is referred to as *equal-priority*. Function `neighbor( $n$ )` will return the list of all nodes (excluding  $n$ ) that have a common successor with  $n$ .

### 3.4 Multi-level Cache-oblivious Partitioning

Here we address the problem of finding a schedule that is cache-size oblivious, and in particular suitable for multi-level memory hierarchy. In order to address this problem, we construct a hierarchical partitioning using the multi-level component growing heuristic shown in Algorithm 5. This algorithm combines individual components formed for a cache of size  $C$  using the heuristic in Algorithm 1 to form components for a cache of size factor  $\ast C$ . In this approach, each component of the partition built at level  $l$  of the heuristic is seen as a single node at level  $l + 1$ . We call these nodes “macro-nodes” as they typically represent sets of nodes in the original CDAG.

This approach could be compared with multi-level tiling for multi-level cache hierarchy, a classical scheme to optimize data locality for multi-level caches. For the first level of this heuristic, a macro-node corresponds to a node in the original CDAG. The heuristic then proceeds with the next level, seeing each component of the partition at the previous level as a macro-node at the current level. The heuristic stops when only one component is generated at the current level, that is, all macro-nodes were successfully added to a single convex component without exceeding the input/output set size constraints. The number of levels in the multi-level partitioning varies with each CDAG, and is not controlled by the user. When a component  $cc_0$  formed at a lower level is added to the current component  $cc_1$  being formed at a higher level, the *liveset* of  $cc_1$  has to be updated, just as if all the nodes composing  $cc_0$  have been added

---

**ALGORITHM 4:** selectBestNode( $R, cc, priority, n$ )

---

**Input** :  $R$ : List of ready nodes  
           $cc$ : current convex component  
           $priority$ : Give priority to neighbor or successor  
           $n$ : Latest node added in the partition

**InOut** :  $cc.readyNeighbors$  : Ready neighbors of current growing partition nodes  
           $cc.readySuccessors$  : Ready successors of current growing partition nodes

**Output**:  $next$  : Next node to add in the partition

**begin**

```
  for  $a \in neighbors(n) \cap R - cc.readyNeighbors$  do
     $cc.readyNeighbors.enqueue(a)$ 
  for  $a \in successors(n) \cap R - cc.readySuccessors$  do
     $cc.readySuccessors.enqueue(a)$ 
   $cc.readyNeighbors \leftarrow cc.readyNeighbors - n$ 
   $cc.readySuccessors \leftarrow cc.readySuccessors - n$ 
  if  $cc.takenNeighbors < cc.takenSuccessors \times priority$ 
     $\wedge cc.readyNeighbors \neq \emptyset$  then
     $next \leftarrow dequeue(cc.readyNeighbors)$ 
     $cc.takenNeighbors \leftarrow cc.takenNeighbors + 1$ 
  else if  $cc.readySuccessors \neq \emptyset$  then
     $next \leftarrow dequeue(cc.readySuccessors)$ 
     $cc.takenSuccessors \leftarrow cc.takenSuccessors + 1$ 
  else
     $next \leftarrow selectReadyNode(R)$ 
  return  $next$ 
```

---

to  $cc_1$ . This leads to the modified version of  $updateLiveSet(p, n, C)$  reported in Algorithm 6, where the function  $FirstLevelBaseNodes(np)$  returns the actual CDAG nodes (that we call first level base nodes) the macro-node  $np$  is built upon. At the first level  $FirstLevelBaseNodes(np)$  may be understood as returning just  $np$ .

**Complexity Analysis** The overall complexity of the single-level version is thus linear with the size of the trace. The multi-level version is run  $\log_{factor} \left( \frac{|M|}{|C|} \right)$  times  $GenerateConvexComponents$ , thus leading to an overall time complexity of  $O(|T| \log(|M|))$ . A step-by-step analysis of the complexity of our analysis can be found in [12].

## 4 Experimental Results

The experimental results are organized in two major parts. In Sec. 4.2 we evaluate the impact of the various parameters of the convex partitioning heuristics, using two well understood benchmarks: matrix multiplication and a 2D Jacobi stencil computation. With these benchmarks, it is well known how the data locality characteristics of the computations can be improved via loop tiling. The goal therefore is to assess how the reuse distance profiles after dynamic analysis and operation reordering compares with the unoptimized untiled original code as well as the optimized tiled version of code.

In Sec. 4.3 we detail several case studies where we use dynamic analysis to characterize the locality potential of several benchmarks for which the state-of-the-art optimizing compilers are unable to automatically optimize data locality. We demonstrate the benefits of dynamic analysis in providing insights into the inherent data locality properties of these computations and the potential for data locality enhancement. Finally we discuss in Sec. 4.4 the sensitivity of our techniques to varying datasets.

---

**ALGORITHM 5:** MultiLevelPartitioning( $G, C, Priority, factor$ )

---

**Input** :  $G$  : CDAG  
           $C$  : initial cache Size  
           $Priority$  : priority to Neighbor or Successor  
           $factor$  : multiplication factor of Cache size for each level  
**InOut** :  $G.M$  : memory footprint of the CDAG  
**Output**:  $P$  : Final single partition  
**begin**  
     $P \leftarrow \text{GenerateConvexComponents}(G, C, Priority)$   
    **while**  $C < G.M$  **do**  
         $G' \leftarrow \text{formMacroNodeWithEachPartition}(P, G)$   
         $C \leftarrow factor * C$   
         $P' \leftarrow \text{GenerateConvexComponents}(G', C, Priority)$   
         $P \leftarrow P'$   
    **return**  $P$

---

---

**ALGORITHM 6:** updateLiveSet( $p, n, C$ )

---

**Input** :  $n$  : New macro-node added in the partition  $p$   
**InOut** :  $p.liveset$  : Live set of  $p$   
**Output**: true if  $|p.liveset| \leq C$ , false otherwise  
**begin**  
     $b \leftarrow \text{true}$   
     $plset \leftarrow p.liveset$   
    **for**  $nb \in \text{FirstLevelBaseNodes}(n)$  **do**  
         $b \leftarrow b \wedge \text{updateLiveSet}(p, nb, C)$   
    **if**  $b = \text{false}$  **then**  
         $p.liveset \leftarrow plset$   
        **return** false  
    **return** true

---

## 4.1 Experimental Setup

The dynamic analysis we have implemented involves three steps. For the CDAG Generation, we use automated LLVM-based instrumentation to generate the sequential execution trace of a program, which is then processed to generate the CDAG. The trace generator was previously developed for performing dynamic analysis to assess vectorization potential in applications [17]. For the convex partitioning of the CDAG, we have implemented the algorithms explained in detail in the previous section. Finally for the reuse distance analysis of the reordered address trace after convex partitioning, it is done using a parallel reuse distance analyzer PARDA [32] that was previously developed.

The total time taken to perform the dynamic analysis is dependent on the input program trace size. In our experiments, computing the trace and performing the full dynamic analysis can range between seconds for benchmarks like Givens, Householder, odd-even sort or Floyd-Warshall to about one hour for SPEC benchmarks such as 420.LBM. For instance, for Givens rotation (QR decomposition) the trace is built in 4 seconds, the analysis takes another 14 seconds, and computing the reuse distance analysis on the partitioned graph takes well below a second. We note that while CDAGs are often program-dependent, the shape of the CDAG and the associated dynamic analysis reasoning can usually be performed on a smaller problem size: the conclusion about the data locality potential is likely to hold for the same program running on larger datasets. A study of the impact of the sensitivity of our analysis to different datasets is provided in later Sec. 4.4. All performance experiments were done on an Intel Core i7 2700K, using a single core.

## 4.2 Impact of Heuristic Parameters

The convex partitioning heuristic takes two parameters. First the *Search Strategy*: this includes (a) prioritization in selecting a new vertex to include in a convex partition: depth-priority, breadth-priority, or alternation between depth and breadth priority (equal priority); and (b) single level partitioning versus multi-level partitioning. The second is *Maxlive*: the parameter that sets a limit on the maximum number of live vertices allowed while forming a partition.

### 4.2.1 Jacobi 2D

Fig. 7 presents the results of applying the dynamic analysis on a Jacobi stencil on a regular 2-dimensional grid of size 32, and 30 time iterations.

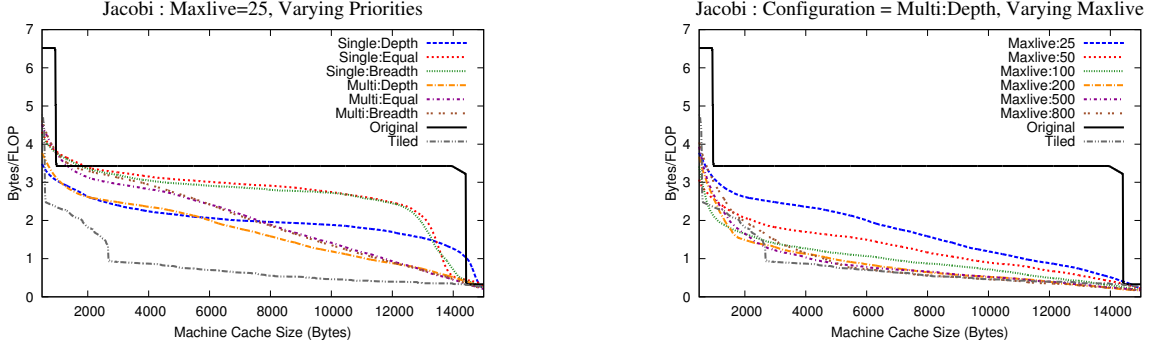


Fig. 7: Results with different heuristics for Jacobi-2D

Fig. 7-left shows reuse distance profiles for a fixed value of *Maxlive* and different configurations for single versus multi-level partitioning, and different priorities for next node selection. With single-level partitioning, depth-priority is seen to provide the best results. Using multi-level partitioning further improves the reuse distance profile. In order to judge the effectiveness of the convex partitioning in improving the reuse distance profile, we show both the reuse distance profiles for the original code and an optimally tiled version of the Jacobi code. It can be seen that there is significant improvement over the original code, but still quite some distance from the profile for the tiled code. Fig. 7-right shows the effect of varying *Maxlive* from 25 to 800, with multi-level depth-priority partitioning.

Here it can be seen that at large values of *Maxlive*, the profile is very close to that of the optimized tiled code. Thus, with a large value of *Maxlive* and use of multi-level depth-priority partitioning, the convex partitioning heuristic is very effective for the Jacobi-2D benchmark.

### 4.2.2 Matrix Multiplication

Fig. 8 shows experimental results for matrix multiplication, for matrices of size 30 by 30. In Fig. 8-left, the selection priority is varied, for single and multi-level partitioning. In contrast to the Jacobi benchmark, for Matmult, equal priority works better than breadth or depth priority. Further, single level partitioning provides better results than multi-level partitioning. In Fig. 8-right, we see performance variation as a function of *Maxlive* for single-level equal-priority partitioning. Again the trends are quite different from those of Jacobi-2D: the best results are obtained with the lowest value of 25 for *Maxlive*.

These results suggest that no single setting of parameters for the convex partitioning heuristic is likely to be consistently effective across benchmarks. We conjecture that there may be a relationship between graph properties of the CDAGs (e.g., low fan-out vs. high fan-out) and the best parameters for the partitioning heuristic.

profile than the best reported heuristic in Fig. 8. This may happen when the tiled implementation achieves the provably optimal I/O lower bound, which is the case for Matmult here. Our heuristics for building convex partitions use several simplifications to improve scalability, in particular in the choice of candidates to be inserted in a partition, and in scheduling the obtained partitions. In addition, we do not explore the Cartesian product of all possible parameters values (priority and maxlive values) but instead limit to a reasonable subset for scalability purposes. All these factors

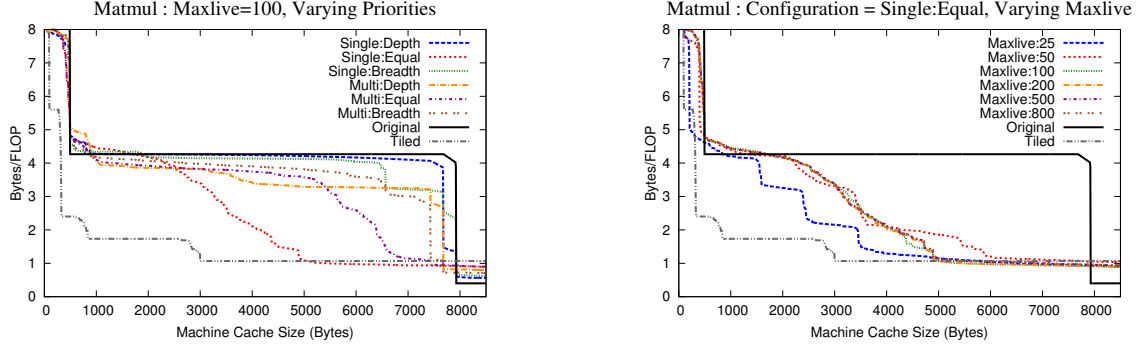


Fig. 8: Results with different heuristics for matrix multiplication

contribute to our analysis possibly under-estimating the data locality potential of the application. We discuss in Sec. 6 the tightness of our analysis and what complementary techniques could be used to assess the quality of our heuristics.

### 4.3 Case Studies

We next present experimental results from applying dynamic analysis to several benchmarks: the Floyd-Warshall algorithm to find all-pairs shortest path in a graph represented with an adjacency matrix, two QR decomposition methods: the Givens rotation and the Householder transformation, three SPEC benchmarks, a LU decomposition code from the LAPACK package, and an implementation of odd-even sorting using linked list. None of these benchmarks could be fully tiled for enhanced data locality by state-of-the-art research compilers (e.g., Pluto [35]) or by production compilers (e.g., Gnu GCC, Intel ICC). For each benchmark, we study the reuse distance profile of the original code and the code after convex partitioning. Where significant potential for data locality enhancement was revealed by the dynamic analysis, we analyzed the code in greater detail. For two of the four benchmarks we manually optimized (namely, Floyd-Warshall and Givens rotation) have static control-flow. Therefore, the performance for these will be only a function of the dataset size and not the content of the dataset. For all optimized benchmarks, we report performance on various dataset sizes (and various datasets when relevant).

#### 4.3.1 Floyd-Warshall

**Original program** We show in Fig. 9 the original input code that we used to implement the Floyd-Warshall algorithm. We refer to this code as “out-of-place” Floyd-Warshall because it uses a temporary array to implement the all-pairs shortest path computation.

```

for (k = 0; k < N; k++) {
  for (i = 0; i < N; i++)
    for (j = 0; j < N; j++)
      temp[i][j] = MIN(A[i][j], (A[i][k] + A[k][j]));
  k++;
  for (i = 0; i < N; i++)
    for (j = 0; j < N; j++)
      A[i][j] = MIN(temp[i][j], (temp[i][k] + temp[k][j]));
}

```

Fig. 9: Floyd-Warshall all-pairs shortest path

**Analysis** Fig. 10-left shows the reuse distance profile of the original code, and the best convex-partitioning found by our heuristics for the Floyd-Warshall algorithm, for a matrix of size 30 by 30. Since the convex-partitioning heuristic shows significantly better reuse distance profile than the original code, there is potential for improvement of data

locality through transformations for this program. Studies on the impact of the various heuristic parameters on the quality of the convex partitioning obtained can be found in [12].

Indeed, the Floyd-Warshall algorithm is immediately tilable, along the two loops  $i$  and  $j$ . Such tiling can for instance be achieved automatically with polyhedral model based compilers such as Pluto [7]. Since the three loops are not fully permutable, it has been believed that the Floyd-Warshall code cannot be 3D-tiled without transformations using semantic properties of the algorithm to create a modified algorithm (i.e., with a different CDAG) that provably produces the same final result [34, 47]. However, a careful inspection of the convex partitions revealed that *valid 3D tiles can be formed among the operations of the standard Floyd-Warshall algorithm*. This non-intuitive result comes from the non-rectangular shape of the tiles needed, with varying tile size along the  $k$  dimension as a function of the value of  $k$ . This motivated us to look for possible transformations that could enable 3D tiling of the code without any semantic transformations.

**Modified implementation** The modified implementation we designed can be found in [12]. It has an identical CDAG, i.e., it is semantically equivalent, to the code in Listing 9. To create this version, we first split the original iteration space into four distinct regions through manual index splitting, followed by tiling of each loop nest.

**Performance comparison** Fig. 10 compares the performance of the tiled version against the original code. From the left plot in Fig. 10, we can observe that the tiled code is able to achieve better data locality, that is close to the potential uncovered by the convex partitioning heuristics. The right plot in Fig. 10 shows the improvement in actual performance of our tiled code (3D tiled - Ours), due to reduced cache misses. A performance improvement of about  $1.6\times$  (sequential execution) is achieved, across a range of problem sizes. Further, to the best of our knowledge, this is the first development of a tiled version of the standard Floyd-Warshall code that preserves the original code’s CDAG. We also compared with the performance achieved by the semantically modified 3D-tiled implementation from [47] and found it to have slightly lower performance.

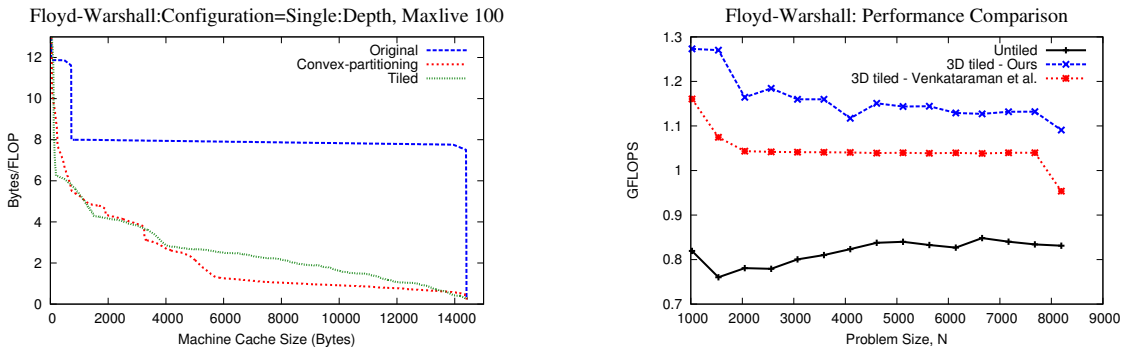


Fig. 10: Floyd-Warshall: Analysis and performance improvements due to tiling

#### 4.3.2 Givens Rotation

**Original program** Fig. 11 shows the original input code for the Givens rotation method used for QR decomposition.

**Analysis** Fig. 13 shows the reuse distance profile of the original code and after convex-partitioning for the Givens rotation algorithm, for an input matrix of size 30 by 30. Studies on the impact of the various heuristic parameters on the quality of the convex partitioning obtained can be found in [12].

The convex partitioning analysis shows good potential for data locality improvement. Similarly to Floyd-Warshall, this code can be automatically tiled by a polyhedral-based compiler [7], after implementing simple loop normalization techniques. However, this is not sufficient to tile all dimensions. Subsequent transformations are needed, as shown below.



```

for (j = 0; j < N; j++) {
  for (i = M-2; i >= j; i--) {
    double c = A[i][j] / sqrt(A[i][j]*A[i][j] + A[i+1][j]*A[i+1][j]);
    double s = -A[i+1][j] / sqrt(A[i][j]*A[i][j] + A[i+1][j]*A[i+1][j]);
    for (k = j; k < N; k++) {
      double t1 = c * A[i][k] - s * A[i+1][k];
      double t2 = s * A[i][k] + c * A[i+1][k];
      A[i][k] = t1;
      A[i+1][k] = t2;
    }
  }
}

```

Fig. 11: Givens Rotation

**Modified implementation** Based on the indicated potential for data locality enhancement, the code in Listing 11 was carefully analyzed and then manually modified to enhance the applicability of automated tiling techniques. Fig. 12 shows this modified version.

```

for (j = 0; j < N; j++) {
  for (i = 0; i <= M-2 - j; i++) {
    c[i][j] = A[(M-2) - (i)][j] / sqrt(A[(M-2) - (i)][j]*A[(M-2) - (i)][j]
    + A[(M-2) - (i)+1][j]*A[(M-2) - (i)+1][j]);
    s[i][j] = -A[(M-2) - (i)+1][j] / sqrt(A[(M-2) - (i)][j]*A[(M-2) - (i)][j]
    + A[(M-2) - (i)+1][j]*A[(M-2) - (i)+1][j]);
    for (k = j; k < N; k++) {
      A[(M-2) - (i)][k] = c[i][j] * A[(M-2) - (i)][k] - s[i][j] * A[(M-2) - (i)+1][k];
      A[(M-2) - (i)+1][k] = s[i][j] * A[(M-2) - (i)][k] + c[i][j] * A[(M-2) - (i)+1][k];
    }
  }
}

```

Fig. 12: Modified Givens Rotation before tiling

It was obtained by first applying loop normalization [21] which consists in making all loops iterate from 0 to some greater value while appropriately modifying the expressions involving the loop iterators within the loop body. Then, we applied scalar expansion on  $c$  and  $s$  [21] to remove dependences induced by those scalars which make loop permutation illegal. As a result, the modified code is an affine code with fewer dependences, enabling it to be automatically tiled by the Pluto compiler [35]. The final tiled code obtained, with default tile-sizes, can be found in [12].

**Performance comparison** Fig. 13-left shows the improvements in the reuse distance profile using the convex partitioning heuristics and the improved reuse distance profile of the tiled code. A better profile is obtained for the tiled version than for convex partitioning. Similarly to Matmult, this is because our convex partitioning heuristic makes simplification for scalability and is therefore not guaranteed to provide the best achievable reuse profile.

Fig 13-right shows a two-fold improvement in the performance of the transformed code for a matrix of size 4000.

#### 4.3.3 Householder Transformation

**Original program** Fig. 14 shows the original input code for the Householder transform, another approach for QR decomposition.

Comparing this with Givens (a different approach to compute the QR decomposition) in terms of data locality potential is of interest: if one has better locality potential than the other, then it would be better suited for deployment on machines where the data movement cost is the bottleneck. It complements complexity analysis, which only characterizes the total number of arithmetic operations to be performed. Indeed, on hardware where the computation power has become increasingly cheaper relative to data access costs, standard complexity analysis alone is insufficient to capture the relative merits of alternative algorithms for a computation such as QR decomposition.

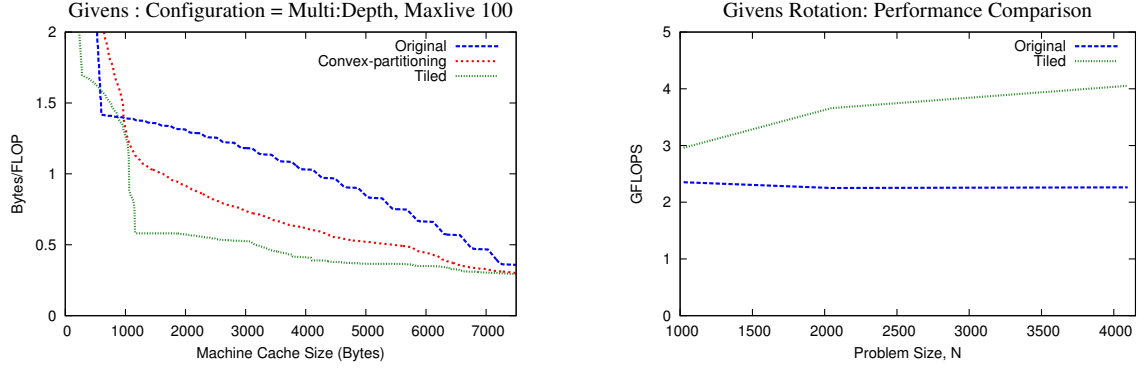


Fig. 13: Givens Rotation: performance improvements due to tiling

```

for (j = 0; j < N; j++) {
    total = 0;
    for (i = j+1; i < M; i++) {
        total += A[i][j] * A[i][j];
    }
    norm_x = (A[j][j] * A[j][j] + total);
    if (norm_x != 0) {
        if (A[j][j] < 0)
            norm_x = -norm_x;
        v[j] = norm_x + A[j][j];
        norm_v = (v[j] * v[j] + total);
        v[j] /= norm_v;
        for (i = j+1; i < M; i++) {
            v[i] = A[i][j] / norm_v;
        }
        for (jj = j; jj < N; jj++) {
            dot = 0.;
            for (kk = j; kk < M; kk++) {
                dot += v[kk] * A[kk][jj];
            }
            for (ii = j; ii < M; ii++) {
                A[ii][jj] -= 2 * v[ii] * dot;
            }
        }
    }
}

```

Fig. 14: Householder computation

**Analysis** Fig. 15 shows the reuse distance profile of the original code and the convex-partitioning for the Householder algorithm, for an input matrix of size 30 by 30.

We observe a significant difference compared with Givens: the gap between the reuse distance profile of the original code and that found by our dynamic analysis is negligible. From this we conclude that the potential for data locality improvement of this algorithm is limited, and therefore we did not seek an optimized implementation for it.

Furthermore, comparing the bytes/flop required with the Givens graph in Fig. 13-left shows that our tiled implementation of Givens achieves a significantly lower byte/flop ratio, especially for small cache sizes. We conclude that the Givens rotation algorithm may be better suited for deployment on future hardware, because of its lower bandwidth demand than Householder, especially for small cache sizes.

#### 4.3.4 Lattice-Boltzmann Method

**Original program** *470.lbm*, a SPEC2006 [16, 36] benchmark, implements the Lattice-Boltzmann technique to simulate fluid flow in 3 dimensions, in the presence of obstacles. The position and structure of the obstacles are known only at run-time, but do not change throughout the course of the computation.

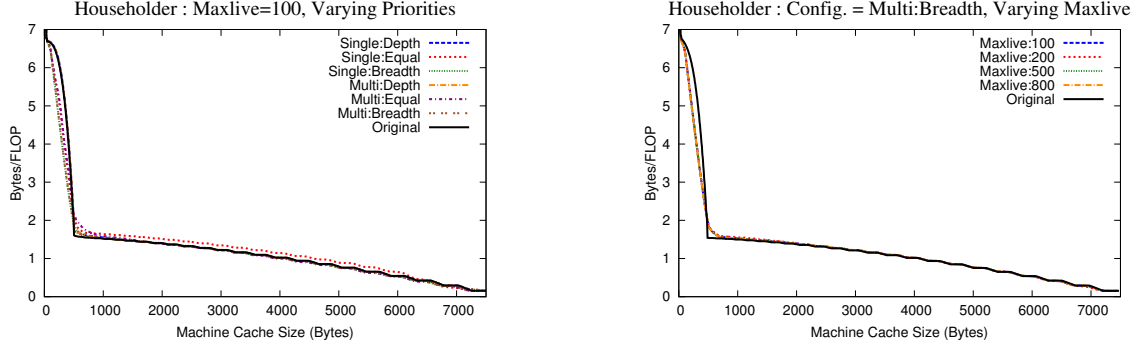


Fig. 15: Results with different heuristics for Householder

**Analysis** The convex-partition heuristics account for the data dependent behavior of the computation and are able to find valid operation reordering with enhanced data locality, as shown Fig. 16. The *test* input size provided by the SPEC benchmark suite was used for the analysis. To reduce the size of the generated trace the problem size was reduced by a factor of 4 along each dimension. The reduced problem still has the same behavior as the original problem.

For a cache size of 60KB, the reordering after convex partitioning obtained by the heuristics show an improvement in the Bytes/FLOP ratio. For this benchmark all configurations of the heuristics yield essentially identical results. However, unlike the previous benchmarks, the absolute value of the bytes/flop is extremely low (Fig. 16), indicating that the computation is already compute-bound and a tiled version of the code would not be able to achieve significant improvements in performance over the untiled code. On an Intel Xeon E5640 with a clock speed of 2.53GHz, the untiled version already achieves a performance of 4GFLOPS. But since the current trend in hardware architecture suggests that the peak performance will continue to grow at a faster rate than the increase in main-memory bandwidth, it is reasonable to expect that optimizations like tiling that improve data locality will be critical in the future even for such computations that are currently compute-bound.

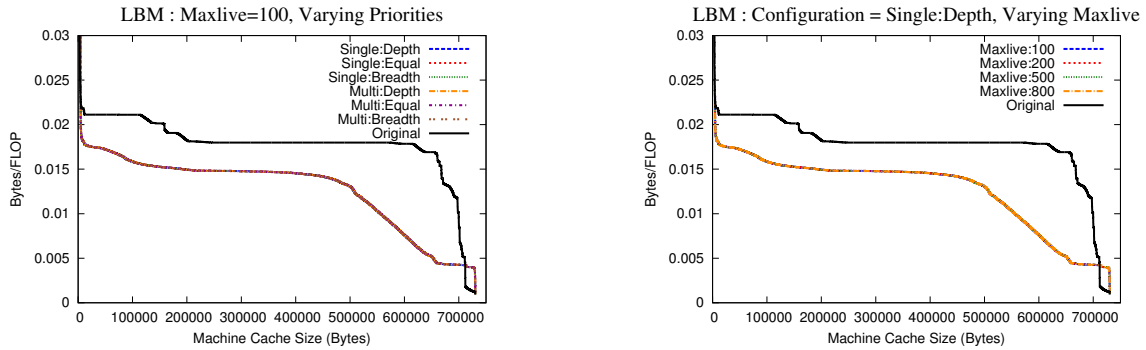


Fig. 16: Results with different heuristics for 470.lbm

#### 4.3.5 410.bwaves

This benchmark is a computational fluid dynamic application from SPEC2006 [16]. We ran our analysis on the whole benchmark with *test* input size. For this benchmark too, the size of the problem was reduced by a factor of 4 along each dimension. The result of the analysis, shown in Fig. 17, indicate a limited potential for improving data locality.

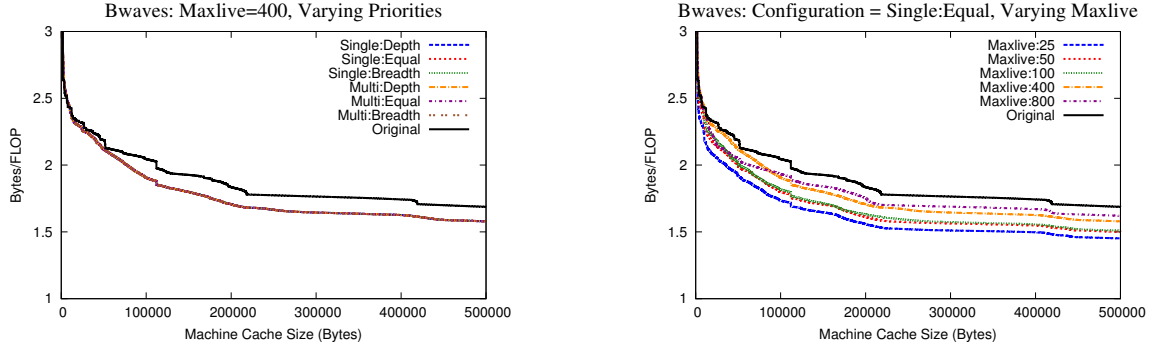


Fig. 17: Results with different heuristics for 410.bwaves

#### 4.3.6 Large-Eddy Simulations with Linear-Eddy Model in 3D

437.leslie3d is another computational fluid dynamic benchmark from SPEC2006 [16]. Here too, the analysis was done using the *test* dataset as given. As shown in Fig. 18, leslie3d achieves a lower bytes/FLOP ratio with the multi-level algorithm. The trend is not sensitive to varying Maxlive. Therefore, from the results, we conclude that this benchmark has high potential for locality improvement. We however leave for future work the task of deriving an optimized implementation for leslie3d.

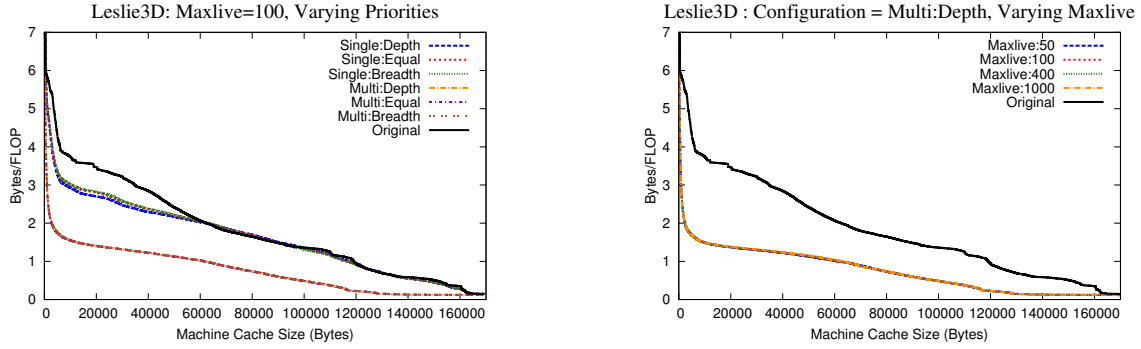


Fig. 18: Results with different heuristics for 437.leslie3d

#### 4.3.7 Odd-Even Sort

**Original program** Our dynamic analysis does not impose any requirement on the data layout of the program: arrays, pointers, structs etc. are seamlessly handled as the trace extraction tool focuses exclusively on the address used in memory read/write operations. To illustrate this we show in Fig. 19 the original code for an odd-even sorting algorithm, using a linked-list implementation. `CompareSwap` compares the data between two consecutive elements in the list, and swaps them if necessary. Each swap operation is represented by a node in the CDAG.

```
for(i=0; i<N/2; ++i) {
    node *curr;
    for(curr=head->nxt; curr->nxt; curr=curr->nxt->nxt) {
        CompareSwap(curr, curr->nxt);
    }
    for(curr=head; curr; curr=curr->nxt->nxt) {
        CompareSwap(curr, curr->nxt);
    }
}
```

Fig. 19: Odd-Even sort on linked list

**Analysis** We have performed our analysis on the original code, for a input list of size 256, with random values. The profile of the original, best convex partitioning (obtained with the best set of heuristic parameters for this program) and tiled (our modified) implementation are shown shown in the left plot in Fig. 20. More complete analysis of the various heuristic parameters result can be found in [12].

**Modified implementation** Based on careful analysis of the original code in Fig. 19, an equivalent register-tiled version with a tile size of 4 was manually developed. It can be found in [12].

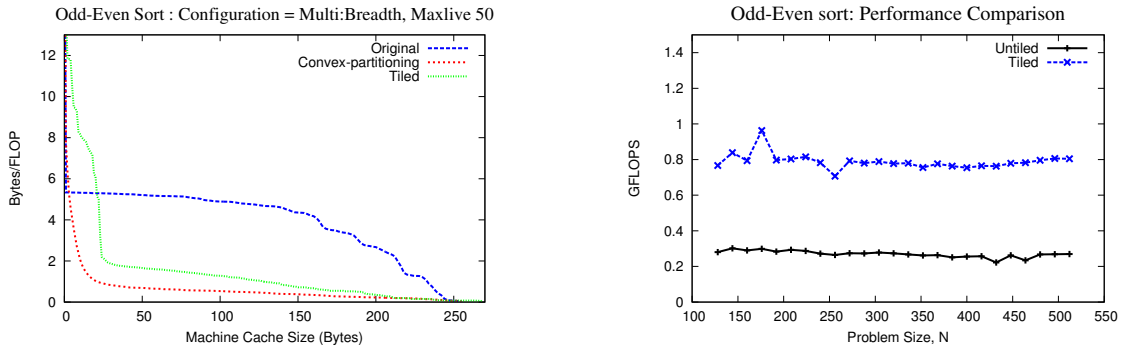


Fig. 20: Odd-Even sort: Performance improvements due to tiling

**Performance comparison** The comparison of performance of the untiled and tiled versions of the code is shown in Fig. 20. The left plot shows the improved data locality for the tiled code compared to the original code. The actual improvement in performance of the tiled code is shown in the right plot in Fig. 20 for a random input. Experiments about sensitivity to datasets reported in later Sec. 4.4 confirm that our optimized variant consistently outperform the original code.

#### 4.3.8 LU Decomposition (LAPACK)

The last benchmark we analyze is an implementation of the LU decomposition for dense matrices, from the LAPACK package [1]. It uses pivoting (therefore the computation is input-dependent) and LAPACK provides both a base

implementation meant for small problem sizes, and a block decomposition for large problem sizes [26]. Both code versions can be found in [1].

We have run our dynamic analysis on the non-blocked implementation of LU decomposition, for a single random matrix of size 128 by 128. The results of varying heuristics and maxlive can be found in [12].

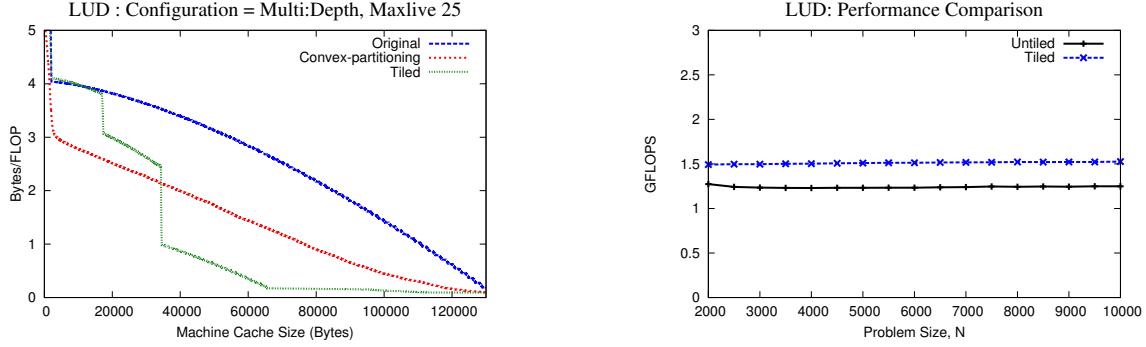


Fig. 21: LU Decomposition

A potential for locality improvement is established from the result of the analysis. On Fig. 21-left, we plot the reuse distance profile of the non-blocked implementation; the convex partitioning with the best heuristic parameters for this program; and tiled (i.e., blocked) implementation, in addition to the original (i.e., non-blocked) one. The blocked version shows a better bytes/Flop than the convex partitioning for cache sizes larger than 35kB. This is likely due to inter-block reuse achieved in the highly optimized LAPACK implementation, combined with a sub-optimal schedule found by our heuristic. Further, Fig. 21-right shows actual performance, in GFLOPS, for non-blocked and blocked versions of the code.

#### 4.4 Dataset Sensitivity Experiments

We conclude our experimental analysis with a study of the sensitivity of our analysis to different datasets. In the set of benchmarks presented in the previous section, the majority of them have a CDAG that depends only on the input dataset size, and not on the input values. Therefore for these codes our dynamic analysis results hold for any dataset of identical size.

Odd-even sort and LUD are two benchmarks that are input-dependent. To determine the sensitivity of the convex-partitioning heuristics on the input, we ran the heuristics on different datasets, as shown in Fig. 22 and Fig. 23.

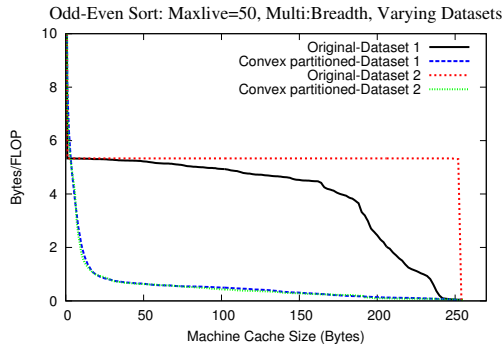


Fig. 22: Sensitivity analysis for odd-even sort

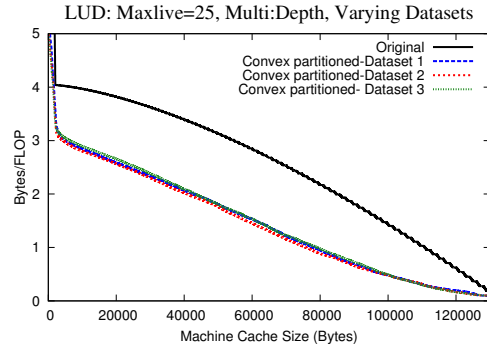


Fig. 23: Sensitivity analysis for LUD

Fig. 22 shows the result for two such datasets - one with random input elements and the other with the reverse sorted input list, a worst-case dataset. We used multi-level heuristics with breadth-first priority, which corresponds

to the parameters of the best result, which can be found in [12]. Fig. 22 shows that the potential for improvement exhibited by the heuristics remains consistent with varying inputs, i.e., the “Convex partitioned” reuse distance profile does not vary with the input value. We note that in the general case, some variations are expected for different datasets. Similar to complexity analysis of such algorithms, one needs to perform both worst-case analysis (i.e., reverse-sorted) and analysis on random/representative datasets for best results.

Fig. 23 exhibits a similar behavior where the three tested datasets have a similar analysis profile. The first dataset has is a random matrix, the second was created so that the pivot changes for about half the rows of the matrix, and for the third one the pivot changes for all rows of the matrix.

Finally, we complete our analysis by reporting in Fig. 24-25 the performance of our manually optimized programs for odd-even sorting and LU decomposition. For two programs (Original, and our modified implementation Tiled), we plot the performance for various datasets (different curves) and various sizes for those datasets (different points on the x axis). We observe very similar asymptotic performance for the various datasets.

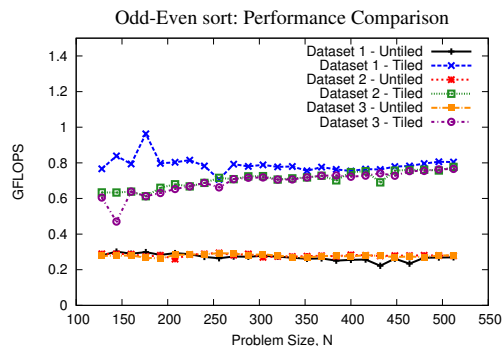


Fig. 24: Performance for odd-even sort

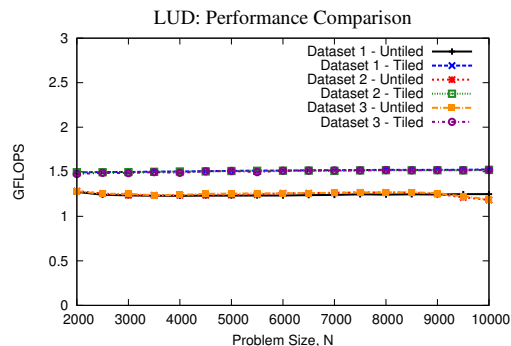


Fig. 25: Performance for LUD

## 5 Related Work

Both algorithmic approaches (e.g., [3, 4, 10]) and compiler transformations (e.g., [7, 18, 22, 49]) have been employed to improve data locality. The applicability of these techniques to arbitrary computations is limited. For example, compiler optimizations typically require programs in which precise static characterization of the run-time behavior is possible; this is challenging in the presence of inter-procedural control flow, diverse data structures, aliasing, etc. Reuse distance analysis [11, 30], which considers the actual observed run-time behavior, is more generally applicable and has been used for cache miss rate prediction [20, 29, 52], program phase detection [42], data layout optimizations [53], virtual memory management [9], and I/O performance optimizations [19]. Even though reuse distance analysis provides insights into the data locality of software behavior, it has been limited to analyzing locality characteristics for a specific execution order of the operations, typically that generated by a sequential program. In contrast to all previous work on reuse distance analysis, to the best of our knowledge, our upper-bounding approach is the first to attempt a schedule-independent characterization of the inherent data locality characteristics of a CDAG.

The idea of considering valid re-orderings of a given execution trace has been applied successfully to characterize the potential parallelism of applications. Kumar’s approach [24] computes a possible valid schedule using a timestamping analysis of an instrumented statement-level execution of the sequential program. Shadow variables are used to store the last modification times for each variable. Each run-time instance of a statement is associated with a timestamp that is one greater than the last-modify times of all its operands. A histogram of the number of operations at each time value provides a fine-grained parallelism profile of the computation, and the maximal timestamp represents the critical path length for the entire computation. Other prior efforts with a similar overall approach include [2, 14, 24, 25, 28, 31, 37, 38, 43, 44, 48].

In contrast to the above fine-grained approach, an alternate technique developed by Larus [27] performed analysis of loop-level parallelism at different levels of a nested loop. Loop-level parallelism is measured by forcing a sequential order of execution of statements within each iteration of a loop being characterized, so that the only available

concurrency is across different iterations of that loop. A related technique is applied in the context of speculative parallelization of loops, where dynamic dependences across loop iterations are tracked [39]. A few recent approaches of similar nature include [8, 33, 45, 46, 50, 51]. In order to estimate parallel speedup of DAGs, Sarkar and Hennessy [40] developed convex partitioning of DAGs. In previous work, we [17] used dynamic analysis of CDAGs to assess the vectorization potential of codes that are not effectively vectorized by current vectorizing compilers. However, we are not aware of any prior work on dynamic analysis of CDAGs with the goal of characterizing and/or enhancing data locality properties of computations.

## 6 Discussion

In this section, we discuss the potential and some of the current limitations of the dynamic analysis approach for data locality characterization/enhancement that we have developed in this article.

**Dependence on Input Values** As with any work that uses dynamic analysis of the actual execution trace of a program, any conclusions drawn are only strictly true for that particular execution. For programs where the execution trace is dependent on input data, the CDAG will change for different runs. Due to space limitations, we only present RDA results for a single problem size for each benchmark. However, we have experimented with different problem sizes and the qualitative conclusions remain stable across problem size. Further, as demonstrated by the case studies of the Floyd-Warshall and Givens rotation codes, the modified codes based on insights from the dynamic analysis were demonstrated to exhibit consistent performance improvement for different problem sizes.

**Overhead of Analysis** The initial prototype implementation of the partitioning algorithm has not yet been optimized and currently has a fairly high overhead (about 4 orders of magnitude) compare to the execution time. As discussed earlier, the computational complexity of the partitioning algorithm is  $O(|T|)$  for the single-level version, and  $O(|T| \log(|M|))$  for the multi-level version and can therefore be made sufficiently efficient to be able to analyze large-scale applications in their entirety.

**Trace Size Limitations** A more significant challenge and limitation of the current system we implemented is the memory requirement. The CDAG size is usually a function of the problem size. For instance, for 470.lbm using the *test* dataset as is would generate a CDAG of size 120GB. The additional data structures used by the tool quickly exhaust the memory on our machines. For instance for 470.lbm we were able to easily create a smaller input dataset (e.g., 1/64th) leading to a 3GB CDAG, that our tool could handle. However, there are numerous benchmarks where such reduction of the input dataset is not possible, and/or does not affect the CDAG size. For those codes, where the CDAG was beyond a few GBs, our current implementation fails due to insufficient memory. The development of an “out-of-core” analyzer is the focus of ongoing follow-up work. Another solution is to compress the CDAG using a technique similar to trace compression [23] leading to a space complexity of  $O(|M| + |P|)$  in the most favorable scenario (in which all dependences turn out to be affine). More generally trace sampling techniques can be applied to tackle scalability issues of this approach.

**Tightness of Estimation** The primary goal of our CDAG partitioning algorithm is to find a more favorable valid reordering of the schedule of its operations so as to lower the volume of data movement between main memory and cache. From the perspective of data movement, the lowest possible amount, which corresponds to the best possible execution order for a given CDAG and a given cache size, can be considered the *inherent data access complexity* of that computation. Irrespective of how much lower the reordered schedule’s data movement volume is compared to the original schedule’s data movement volume, how do we determine how close we are to the best possible valid order of execution? A possible solution is to work from the opposite direction and develop lower bound techniques for the data access complexity of CDAGs. In a complementary work we are developing an approach to establishing lower bounds on the data movement costs for arbitrary CDAGs. One way of assessing the tightness of the upper bounds (this work) and lower bounds (complementary work in progress) is to see how close these two bounds are for a given CDAG.



**Use of Analysis** We envision several uses of a tool based on the dynamic analysis approach developed in this paper. (1) *For Application Developers*: By running the dynamic analysis on different phases of an application, along with standard performance profiling, it is possible to identify which of the computationally dominant phases of the application may have the best potential for performance improvement through code changes that enhance data reuse. Dynamic analysis for data locality can also be used to compare and choose between alternate equivalent algorithms with the same functionality – even if they have similar performance on current machines. If the reuse distance profiles of two algorithms after reordering based on dynamic analysis are very different, the algorithm with lower bandwidth demands would likely be better for the future. (2) *For Compiler Developers*: Compilers implement many transformations like fusion and tiling that enhance data reuse. The results from the convex partitioning of the CDAG can be used to gauge the impact of compiler transformations and potential for improvement. (3) *For Architecture Designers*: Running the dynamic analysis tool on a collection of representative applications can guide vendors of architectures in designing hardware that provides adequate bandwidth and/or sufficient capacity for the different levels of the memory hierarchy.

## 7 Conclusion

With future systems, the cost of data movement through the memory hierarchy is expected to become even more dominant relative to the cost of performing arithmetic operations [5, 13, 41], both in terms of throughput and energy. Therefore optimizing data locality will become ever more critical in the coming years. Given the crucial importance of optimizing data access costs in systems with hierarchical memory, it is of great interest to develop tools and techniques for characterization and enhancement of the data locality properties of an algorithm. Although reuse distance analysis [11, 30] provides a useful characterization of data locality for a given execution trace, it fails to provide any information on the potential for improving the in data reuse through valid reordering of the operations in the execution trace.

In this paper, we have developed a dynamic analysis approach to provide insights beyond what is possible from standard reuse distance analysis. Given an execution trace from a sequential program, we seek to (i) characterize the data locality properties of an algorithm and (ii) determine if there exists potential for enhancement of data locality through execution reordering. Since we first explicitly construct a dynamic computational directed acyclic graph (CDAG) to capture the statement instances and their inter-dependences; perform convex partitioning of the CDAG to generate a modified, dependence-preserving, execution order with better expected data reuse; and then perform reuse distance analysis on the trace corresponding to the modified execution order, we expect to get a better characterization of the potential benefit of reordering. We have demonstrated the utility of the approach in characterizing/enhancing data locality for a number of benchmarks.

## References

- [1] E. Anderson, Z. Bai, C. Bischof, S. Blackford, J. Demmel, J. Dongarra, J. Du Croz, A. Greenbaum, S. Hammarling, A. McKenney, and D. Sorensen. *LAPACK Users' Guide*. Society for Industrial and Applied Mathematics, Philadelphia, PA, third edition, 1999.
- [2] Todd Austin and Gurindar Sohi. Dynamic dependency analysis of ordinary programs. In *ISCA*, pages 342–351, 1992.
- [3] G. Ballard, J. Demmel, O. Holtz, and O. Schwartz. Minimizing communication in numerical linear algebra. *SIAM Journal on Matrix Analysis and Applications*, 32(3):866–901, 2011.
- [4] Grey Ballard, James Demmel, Olga Holtz, and Oded Schwartz. Graph expansion and communication costs of fast matrix multiplication: regular submission. In *Proc. SPAA*, pages 1–12, New York, NY, USA, 2011. ACM.
- [5] K. Bergman, S. Borkar, et al. Exascale computing study: Technology challenges in achieving exascale systems. *DARPA IPTO, Tech. Rep*, 2008.

- [6] G. Bilardi and E. Peserico. A characterization of temporal locality and its portability across memory hierarchies. *Proc. ICALP*, pages 128–139, 2001.
- [7] Uday Bondhugula, Albert Hartono, J. Ramanujan, and P. Sadayappan. A practical automatic polyhedral parallelizer and locality optimizer. In *Proc. PLDI*, 2008.
- [8] Matthew Bridges, Neil Vachharajani, Yun Zhang, Thomas Jablin, and David August. Revisiting the sequential programming model for multi-core. In *MICRO*, pages 69–84, 2007.
- [9] Calin Cascaval, Evelyn Duesterwald, Peter F. Sweeney, and Robert W. Wisniewski. Multiple page size modeling and optimization. In *Proc. PACT*. IEEE Computer Society, 2005.
- [10] J. Demmel, L. Grigori, M. Hoemmen, and J. Langou. Communication-optimal parallel and sequential QR and LU factorizations. *SIAM Journal on Scientific Computing*, 34(1):206–239, 2012.
- [11] Chen Ding and Yutao Zhong. Predicting whole-program locality through reuse distance analysis. In *PLDI*, pages 245–257. ACM, 2003.
- [12] Naznin Fauzia, Venmugil Elango, Mahesh Ravishankar, Louis-Noël Pouchet, J. Ramanujam, Fabrice Rastello, Atanas Rountev, and P. Sadayappan. Beyond reuse distance analysis: Dynamic analysis for characterization of data locality potential. Technical Report OSU-CISRC-9/13-TR19, Ohio State University, September 2013.
- [13] Samuel H. Fuller and Lynette I. Millett. *The Future of Computing Performance: Game Over or Next Level?* The National Academies Press, 2011.
- [14] Saturnino Garcia, Donghwan Jeon, Christopher M. Louie, and Michael Bedford Taylor. Kremlin: Rethinking and rebooting gprof for the multicore age. In *PLDI*, pages 458–469, 2011.
- [15] J.L. Hennessy and D.A. Patterson. *Computer architecture: a quantitative approach*. Morgan Kaufmann, 2011.
- [16] John L. Henning. Spec cpu2006 benchmark descriptions. *SIGARCH Comput. Archit. News*, 2006.
- [17] Justin Holewinski, Ragavendar Ramamurthi, Mahesh Ravishankar, Naznin Fauzia, Louis-Noël Pouchet, Atanas Rountev, and P. Sadayappan. Dynamic trace-based analysis of vectorization potential of applications. In *Proc. PLDI*, pages 371–382, New York, NY, USA, 2012. ACM.
- [18] F. Irigoin and R. Triolet. Supernode partitioning. In *Proc. POPL*, pages 319–329, 1988.
- [19] Song Jiang and Xiaodong Zhang. Making LRU Friendly to Weak Locality Workloads: A Novel Replacement Algorithm to Improve Buffer Cache Performance. *IEEE Trans. Comput.*, 54:939–952, August 2005.
- [20] Yunlian Jiang, Eddy Z. Zhang, Kai Tian, and Xipeng Shen. Is reuse distance applicable to data locality analysis on chip multiprocessors? In *Proc. Comp. Const.*, pages 264–282, 2010.
- [21] K. Kennedy and J. Allen. *Optimizing compilers for modern architectures: A dependence-based approach*. Morgan Kaufmann, 2002.
- [22] Ken Kennedy and Kathryn S. McKinley. Maximizing loop parallelism and improving data locality via loop fusion and distribution. In *Languages and Compilers for Parallel Computing*, pages 301–320. Springer-Verlag, 1993.
- [23] Alain Ketterlin and Philippe Clauss. Prediction and trace compression of data access addresses through nested loop recognition. In *Proc. CGO*, pages 94–103, 2008.
- [24] Manoj Kumar. Measuring parallelism in computation-intensive scientific/engineering applications. *IEEE Transactions on Computers*, 37(9):1088–1098, September 1988.
- [25] M. Lam and R. Wilson. Limits of control flow on parallelism. In *ISCA*, pages 46–57, 1992.

- [26] LAPACK. <http://www.netlib.org/lapack>.
- [27] James Larus. Loop-level parallelism in numeric and symbolic programs. *IEEE Transactions on Parallel and Distributed Systems*, 4(1):812–826, July 1993.
- [28] Jonathan Mak and Alan Mycroft. Limits of parallelism using dynamic dependency graphs. In *WODA*, pages 42–48, 2009.
- [29] Gabriel Marin and John Mellor-Crummey. Cross-architecture performance predictions for scientific applications using parameterized models. In *SIGMETRICS '04/Performance '04*. ACM, 2004.
- [30] R.L. Mattson, J. Gecsei, D. Slutz, and I. L. Traiger. Evaluation techniques for storage hierarchies. *IBM Systems Journal*, 9(2):78–117, 1970.
- [31] A. Nicolau and J. Fisher. Measuring the parallelism available for very long instruction word architectures. *IEEE Transactions on Computers*, 33(11):968–976, 1984.
- [32] Qingpeng Niu, J. Dinan, Qingda Lu, and P. Sadayappan. Parda: A fast parallel reuse distance analysis algorithm. In *Proc. IPDPS*, pages 1284–1294, may 2012.
- [33] Cosmin Oancea and Alan Mycroft. Set-congruence dynamic analysis for thread-level speculation (TLS). In *LCPC*, pages 156–171, 2008.
- [34] Joon-Sang Park, Michael Penner, and Viktor K. Prasanna. Optimizing Graph Algorithms for Improved Cache Performance. *IEEE Transactions on Parallel Distributed Systems*, 15(9):769–782, 2004.
- [35] Pluto: A polyhedral automatic parallelizer and locality optimizer for multicores. <http://pluto-compiler.sourceforge.net>.
- [36] Thomas Pohl. 470.lbm. <http://www.spec.org/cpu2006/Docs/470.lbm.html>.
- [37] Matthew Postiff, David Greene, Gary Tyson, and Trevor Mudge. The limits of instruction level parallelism in SPEC95 applications. *SIGARCH Computer Architecture News*, 27(1):31–34, 1999.
- [38] Lawrence Rauchwerger, Pradeep Dubey, and Ravi Nair. Measuring limits of parallelism and characterizing its vulnerability to resource constraints. In *MICRO*, pages 105–117, 1993.
- [39] Lawrence Rauchwerger and David Padua. The LRPD test: Speculative run-time parallelization of loops with privatization and reduction parallelization. In *PLDI*, pages 218–232, 1995.
- [40] Vivek Sarkar and John L. Hennessy. Compile-time partitioning and scheduling of parallel programs. In *SIGPLAN Symposium on Compiler Construction*, pages 17–26, 1986.
- [41] J. Shalf, S. Dosanjh, and J. Morrison. Exascale computing technology challenges. *High Performance Computing for Computational Science–VECPAR 2010*, pages 1–25, 2011.
- [42] Xipeng Shen, Yutao Zhong, and Chen Ding. Locality phase prediction. In *Proc. ASPLOS*. ACM, 2004.
- [43] Darko Stefanović and Margaret Martonosi. Limits and graph structure of available instruction-level parallelism. In *Euro-Par*, pages 1018–1022, 2000.
- [44] Kevin Theobald, Guang Gao, and Laurie Hendren. On the limits of program parallelism and its smoothability. In *MICRO*, pages 10–19, 1992.
- [45] Chen Tian, Min Feng, Vijay Nagarajan, and Rajiv Gupta. Copy or discard execution model for speculative parallelization on multicores. In *MICRO*, pages 330–341, 2008.
- [46] Georgios Tournavitis, Zheng Wang, Zheng, Björn Franke, and Michael O’Boyle. Towards a holistic approach to auto-parallelization. In *PLDI*, pages 177–187, 2009.

- [47] G. Venkataraman, S. Sahni, and S. Mukhopadhyaya. A Blocked All-Pairs Shortest-Paths Algorithm. *Journal of Experimental Algorithmics*, 8:2.2, December 2003.
- [48] David Wall. Limits of instruction-level parallelism. In *ASPLOS*, pages 176–188, 1991.
- [49] Michael E. Wolf and Monica S. Lam. A data locality optimizing algorithm. In *PLDI '91: ACM SIGPLAN 1991 conference on Programming language design and implementation*, pages 30–44, New York, NY, USA, 1991. ACM Press.
- [50] Peng Wu, Arun Kejariwal, and Caălin Caşcaval. Compiler-driven dependence profiling to guide program parallelization. In *LCPC*, pages 232–248, 2008.
- [51] Hongtao Zhong, Mojtaba Mehrara, Steve Lieberman, and Scott Mahlke. Uncovering hidden loop level parallelism in sequential applications. In *HPCA*, pages 290–301, 2008.
- [52] Yutao Zhong, Steven G. Dropsho, and Chen Ding. Miss rate prediction across all program inputs. In *Proc. PACT*, 2003.
- [53] Yutao Zhong, Maksim Orlovich, Xipeng Shen, and Chen Ding. Array regrouping and structure splitting using whole-program reference affinity. In *Proc. PLDI*. ACM, 2004.